Diameter and Chirality Dependence of Exciton Properties in Carbon Nanotubes

Rodrigo B. Capaz[1,2,5,6], Catalin D. Spataru[3,5,6], Sohrab Ismail-Beigi[4], and Steven G. Louie[5,6]

[1]*Instituto de Física, Universidade Federal do Rio de Janeiro,*
Caixa Postal 68528, Rio de Janeiro, RJ 21941-972, Brazil
[2]*Divisão de Metrologia de Materiais, Instituto Nacional de Metrologia, Normalização e Qualidade Industrial - Inmetro,*
R. Nossa Senhora das Graças 50, Xerém, Duque de Caxias, RJ 25245-020, Brazil
[3]*Center for Integrated Science and Engineering and Center for Electron Transport in Molecular Nanostructures,*
Columbia University, New York, NY 10027, USA
[4]*Department of Applied Physics, Yale University, New Haven, Connecticut 06520, USA*
[5]*Department of Physics, University of California at Berkeley, Berkeley, CA 94720, USA*
[6]*Materials Science Division, Lawrence Berkeley National Laboratory, Berkeley, CA 94720, USA*
(Dated: February 3, 2008)

We calculate the diameter and chirality dependences of the binding energies, sizes, and bright-dark splittings of excitons in semiconducting single-wall carbon nanotubes (SWNTs). Using results and insights from *ab initio* calculations, we employ a symmetry-based, variational method based on the effective-mass and envelope-function approximations using tight-binding wavefunctions. Binding energies and spatial extents show a leading dependence with diameter as $1/d$ and d, respectively, with chirality corrections providing a spread of roughly 20% with a strong family behavior. Bright-dark exciton splittings show a $1/d^2$ leading dependence. We provide analytical expressions for the binding energies, sizes, and splittings that should be useful to guide future experiments.

Diameter and chirality trends are one of the most useful concepts in nanotube science. Often, new physics arises when the diameter and chirality dependences of a given property are fully disclosed. A classic example is the analysis of "family patterns" in optical transitions combined with the diameter dependence of vibrational frequencies that paved the way to reliable (n, m) assignments of single-wall carbon nanotubes (SWNTs) [1] and posed the fundamental "ratio problem" [2]. Therefore, a reliable determination of diameter and chirality trends of a given nanotube property, even when this is accomplished by simplified models, is often as important as determining accurately that property for a limited number of tubes. Moreover, when a reliable model for trends is coupled with an accurate *ab initio* theory that determines its parameters, the model acquires quantitative and predictive powers.

The exciton concept solved the "ratio problem" [3], and it is now widely accepted that the optical spectra of carbon nanotubes are dominated by exciton features [3, 4, 5, 6, 7]. Recent experiments based on two-photon spectroscopy [8, 9, 10] and Raman spectroscopy on electrochemically doped samples [11] have provided the first experimental evaluations of exciton binding energies for a few single-wall carbon nanotubes (SWNTs). However, a full description of diameter and chirality dependences of exciton properties in SWNTs has not yet been provided, neither experimentally nor theoretically. *Ab initio* calculations are restricted to a few small-diameter tubes [3, 5]. Perebeinos *et al.* [6] have extracted scaling relations of binding energies and sizes with diameter from model calculations, but the chirality dependence has not been addressed. Semi-empirical calculations have also been done for a larger variety of tubes [7], but again systematic

diameter and chirality trends have not been extracted. Finally, the important issue of bright-dark exciton splittings have been addressed in detail by considerably fewer calculations [12, 13, 14].

In this work, we calculate the full diameter and chirality dependences of exciton properties in SWNTs. We employ a symmetry-based, variational, tight-binding method, based on the effective mass and envelope function approximations [15, 16]. Since we explictly impose the symmetry of the exciton wavefunction, we can calculate properties of bright and dark excitons. Our model is parametrized by *ab initio* results. We calculate binding energies and sizes for the lowest-energy bright excitons (those usually associated with the E_{11} singularity in the single particle joint density of states), as well as dark-bright exciton splittings for a large number of SWNTs. From these results, we extract reliable analytical expressions for the diameter and chirality dependences of such properties.

Our variational exciton wavefunction is written as:

$$\psi(\vec{r}_e, \vec{r}_h) = C \sum_{v,c} A_{vc} \phi_c(\vec{r}_e) \phi_v^*(\vec{r}_h) e^{\frac{(z_e - z_h)^2}{2\sigma^2}}, \quad (1)$$

where $\phi_c(\vec{r}_e)$ and $\phi_v(\vec{r}_h)$ are conduction (electron) and valence (hole) single-particle states. The sum is restricted to the four band-edge states $c = \pm m$ and $v = \pm m$ from the top of the valence and bottom of the conduction bands. Note that both valence and conduction band edges are 2-fold degenerate for both zigzag and chiral tubes, once time-reversal symmetry is considered [17, 18]. The single-particle wavefunctions are labeled by their quasi-angular momentum quantum numbers $+m$ and $-m$ and they are taken from properly symmetrized wavefunctions of graphene expanded in a π-orbital tight-

TABLE I: Symmetries, degeneracies, optical activities and coefficients A_{vc} for excitons in zigzag and chiral tubes. The symmetries are described by the irreducible representations in both group of the wave vector [18] and line group [17](in parenthesis) notations. The label m' is the quasi-angular momentum quantum number of the double-degenerate exciton.

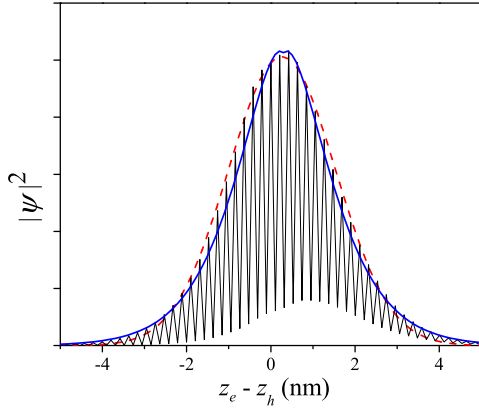| Zigzag						
Symmetry	Deg.	Activity	A_{++}	A_{--}	A_{+-}	A_{-+}
$A_{1u}(_0B_0^-)$	1	dark	1	-1	0	0
$A_{2u}(_0A_0^-)$	1	bright	1	1	0	0
$E_{m',u}(_0E_{m'}^-)$	2	dark	0	0	±1	∓1
Chiral						
Symmetry	Deg.	Activity	A_{++}	A_{--}	A_{+-}	A_{-+}
$A_1(_0A_0^+)$	1	dark	1	1	0	0
$A_2(_0A_0^-)$	1	bright	1	-1	0	0
$\mathbb{E}_{m'}(k)+\mathbb{E}_{-m'}(-k)(_kE_{m'})$	2	dark	0	0	±1	∓1

FIG. 1: (Color online) Lowest-energy singlet exciton wavefunction of the (11,0) tube. Black thin line: *Ab initio* $|\psi|^2$ after integrating out on the coordinates perpendicular to the tube. Red thick dashed line: Envelope fit using a gaussian. Blue thick line: Envelope fit using a Whittaker function. Notice that the two fits are almost indistinguishable.

binding basis. [17] The coefficients A_{vc}, responsible for the quantum interference between pair excitations, are then completely determined by symmetry, as described in Table I.

We choose a gaussian envelope function. This choice is justified both by a fit of the *ab initio* exciton wavefunctions [3], as shown in Fig. 1, and by an analogy with the regularized Coulomb potential problem in 1D [19, 20], for which the ground-state Whittaker function closely resembles a gaussian. The gaussian width or exciton size σ is the only variational parameter in the problem. The constant C normalizes the exciton wavefunction: $\int\int|\psi(\vec{r}_e,\vec{r}_h)|^2d\vec{r}_ed\vec{r}_h=1$.

We minimize the exciton energy that is composed of

three terms: direct, exchange and kinetic energies. Here, we treat singlet excitons only. The direct term is written as:

$$<K^d>=\int\psi^*(\vec{r}_e,\vec{r}_h)V_C^{scr}(\vec{r}_e-\vec{r}_h)\psi(\vec{r}_e,\vec{r}_h)d\vec{r}_ed\vec{r}_h$$
$$=C^2\sum_{vc,v'c'}A_{vc}^*A_{v'c'}\sum_{\vec{R}_1,\vec{R}_2}c_v(\vec{R}_1)c_{v'}^*(\vec{R}_1)c_c^*(\vec{R}_2)c_{c'}(\vec{R}_2)\times$$
$$\times e^{-\frac{(z_1-z_2)^2}{\sigma^2}}U_{Ohno}^{scr}(|\vec{R}_1-\vec{R}_2|),(2)$$

where V_C^{scr} is the screened Coulomb interaction and we wrote the direct energy in terms of the tight-binding expansion coefficients of the single-particle wavefunctions in a p_z-orbital basis $\varphi(\vec{r}-\vec{R}_i)$ centered in the atomic positions $\vec{R}_i$:

$$\phi_n(\vec{r})=\sum_i c_n(\vec{R}_i)\varphi(\vec{r}-\vec{R}_i). \quad (3)$$

The Coulomb integrals between sites are parametrized by the Ohno formula [21]:

$$U_{Ohno}^{scr}(R)=\frac{U_0}{\epsilon\sqrt{(\frac{4\pi\epsilon_0}{e^2}U_0R)^2+1}}. \quad (4)$$

The onsite Coulomb repulsion $U_0=16$ eV and the dielectric constant $\epsilon=1.846$ are chosen to reproduce the *ab initio* values for the binding energy and bright-dark exciton splittings for the (11,0) tube and kept constant for all other tubes. The exchange energy is given by:

$$<K^x>=2\int\psi^*(\vec{r}_e,\vec{r}_e)V_C(\vec{r}_e-\vec{r}_h)\psi(\vec{r}_h,\vec{r}_h)d\vec{r}_ed\vec{r}_h$$
$$=2C^2\sum_{vc,v'c'}A_{vc}^*A_{v'c'}\sum_{\vec{R}_1,\vec{R}_2}c_v(\vec{R}_1)c_c(\vec{R}_1)c_{v'}^*(\vec{R}_2)c_{c'}^*(\vec{R}_2)\times$$
$$\times U_{Ohno}(|\vec{R}_1-\vec{R}_2|).(5)$$

In this case, the unscreened Coulomb interaction V_C is parametrized by taking $\epsilon=1$ in Eq.(4). Finally, the kinetic energy associated with the exciton relative coordinate is simply that of a gaussian envelope:

$$<T>=\frac{\hbar^2}{4m^*\sigma^2}, \quad (6)$$

where the exciton reduced mass m^* is given by $1/m^*=1/m_e+1/m_h$. We use the diameter- and chirality-dependent electron (m_e) and hole (m_h) effective masses obtained from tight-binding calculations [22].

To test our model, we compare in Table II our variational binding energies with *ab initio* ones obtained from solving the Bethe-Salpeter equation [3] for a few zigzag tubes. The agreement is excellent, except for the E_{22} exciton in the (7,0) SWNT. This discrepancy can be understood: For the small-diameter (7,0) tube, the E_{22} exciton size becomes extremely small ($\sigma=5.3$ Å) and therefore

TABLE II: *Ab initio* and model binding energies for bright E_{11} and E_{22} excitons for a few small-diameter SWNTs.

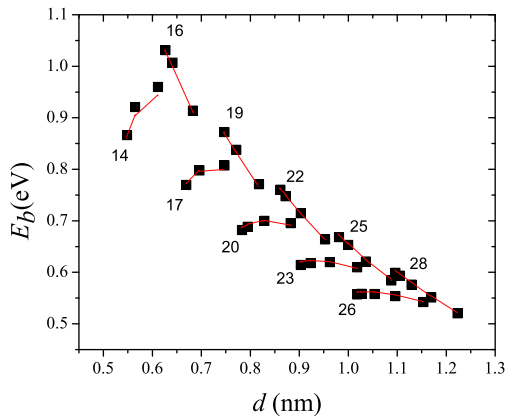| Tube	E_b^{11} (eV)		E_b^{22} (eV)	
	Ab Initio	Model	*Ab Initio*	Model
(7,0)	0.89	0.87	1.13	1.61
(8,0)	0.99	1.03	0.86	0.92
(10,0)	0.76	0.68	0.95	1.09
(11,0)	0.76	0.76 (fitted)	0.72	0.75

FIG. 2: Binding energies for the lowest-energy bright excitons in 38 SWNTs with varying diameter and chirality. The dots are our model results and the red lines represent the analytical fit using Eq.(7). The labels indicate the $(2n+m)$ families.

the envelope-function approximation is not expected to be valid in this regime. Notice also that our model correctly captures the family oscillations in the binding energy.

Fig. 2 shows the binding energy of the E_{11} bright exciton as a function of diameter for 38 SWNTs covering the full range of chiralities. The $(2n+m)$ family indices are indicated in the figure. One clearly sees the well-known family pattern reminiscent from the so-called Kataura plots for optical transition energies. [22] As expected, binding energies decrease with tube diameter. Chirality effects are also strong, contributing to about 20% spread in the binding energies for a given diameter. It is clear that excitons in $(2n+m)$ mod 3 = 1 (MOD1) tubes have generally larger binding energies than in $(2n+m)$ mod 3 = 2 (MOD2) tubes.

Fig. 3 shows the exciton sizes as a function of diameter. Again, as expected, exciton sizes increase with diameter and they show the opposite MOD1-MOD2 trends as compared to binding energies. Notice that even for tubes as small as 0.5 nm in diameter the E_{11} exciton sizes are already several times larger than the carbon-carbon bond, thus justifying the use of the envelope-function approximation.
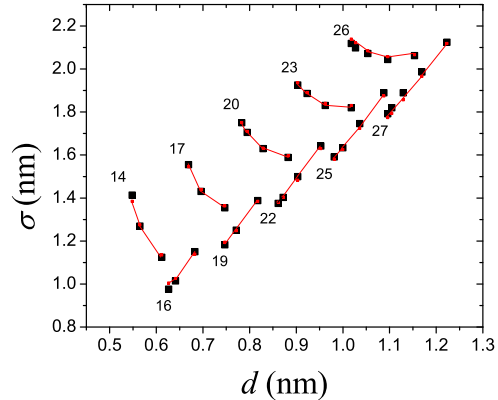

FIG. 3: Sizes of the bright lowest-energy excitons for 38 SWNTs with varying diameter and chirality. The dots are our model results and the red lines represent the analytical fit using Eq.(7). The labels indicate the $(2n+m)$ families.

Analytical expressions for diameter and chirality dependences, although sometimes lacking a deeper physical justification, can be extremely useful for a quick evaluation of a variety of nanotube properties. We succeeded in finding simple yet very accurate analytical approximations for both binding energies and sizes:

$$E_b = \frac{1}{d}\left(A + \frac{B}{d} + C\xi + D\xi^2\right)$$
$$\sigma = d(E + F\xi + G\xi^2), \qquad (7)$$

where d is the tube diameter in nm and $\xi = (-1)^\nu cos3\theta/d$ captures the chirality dependence [23]. The best fits are given by $A = 0.6724$ eV.nm, $B = -4.910 \times 10^{-2}$ eV.nm^2, $C = 4.577 \times 10^{-2}$ eV.nm^2, $D = -8.325 \times 10^{-3}$ eV.nm^3, $E = 1.769$, $F = -2.490 \times 10^{-1}$ nm and $G = 9.130 \times 10^{-2}$ nm^2. These analytical fits are plotted in red lines in Figs. 2 and 3, together with the numerical results. The agreement is nearly perfect.

Our theory also allows for an estimation of chirality and diameter dependences of exciton splittings among exciton states of the ground-state complex of the same E_{ii}. These splittings are fundamental to understand a variety of optical properties of carbon nanotubes, such as the quantum efficiency for light emission and the exciton radiative lifetime [12, 13]. *We find that the lowest-energy exciton for all SWNTs is the singly-degenerate dark state,* due to its vanishing exchange energy [12]. Defining the exciton splittings from the lowest-energy exciton to the bright exciton and to the double-degenerate dark exciton as δ_1 and δ_2, we find the following dependence on diameter and chirality:

$$\delta_i = \frac{1}{d^2}\left(A_i + B_i\xi + C_i d\xi^2\right), \qquad (8)$$

with $A_1 = 18.425$ meV.nm^2, $B_1 = 12.481$ meV.nm^3, $C_1 = -0.715$ meV.nm^3, $A_2 = 32.332$ meV.nm^2, $B_2 = 7.465$ meV.nm^3 and $C_2 = -2.576$ meV.nm^3. So, in disagreement with Perebeinos *et al.* [13], we find the leading dependence of bright-dark splittings to be $1/d^2$. This is precisely the dependence of the exchange energy $< K^x >$ on diameter.

It is instructive to explain on physical grounds the leading dependences on diameter of the exciton sizes, binding energies and the bright-dark splittings. The exciton sizes σ scale like d because the 1D Coulomb potential is smoothed out or regularized over the scale of the tube diameter d and this sets the length scale of the bound state (recall that in a pure 1D system with no lateral size, the Coulomb potential gives a delta-function ground state with infinite binding energy). The binding energies go like $1/d$ because σ scales like d and Coulomb interactions go like inverse distance [6]. The scaling of dark-bright splittings mirrors the scaling of the exchange energy $< K^x >$ which goes like $1/d^2$ because $< K^x >$ is the self-interaction of a neutral charge distribution with dipole moments: The long-range part (from distances larger than d) can be written as $\int_d^\infty dx/x^3 \sim 1/d^2$.

We now compare our results to the available experimental determinations of the exciton binding energies to date. Two-photon spectroscopy have been performed for SWNTs in a polymeric matrix [8, 9] and in D_2O solution wrapped by a surfactant [10]. These environments should provide extra screening, so these results should not be directly compared with *ab initio* theory for isolated tubes. However, in our variational scheme, it is very easy to investigate the influence of screening and to adjust the dielectric constant ϵ to match the experimental results. In fact, we find that binding energies follow very nicely the scaling $E_b \propto \epsilon^{-1.4}$ proposed by Perebeinos *et al.* [6]. Therefore, it is straightforward to apply Eq.(7) for SWNTs in *any* environment, provided that one scales the binding energies by using the appropriate phenomenological dielectric constant. For instance, taking $\epsilon = 3.049$ gives binding energies in excellent agreement (standard deviation of 0.02 eV) for all 13 SWNTs measured by Dukovic *et al.* [9]. Similarly, the results of Maultzsch *et al.* [10] for 6 different SWNTs are reproduced with a standard deviation of 0.03 eV using a slightly larger dielectric constant $\epsilon = 3.208$.

In another recent experiment, Raman spectroscopy under electrochemical doping was used in nanotubes coated with a surfactant to give 0.62 eV and 0.49 eV for the binding energies of excitons associated with E_{22} transitions in the (7,5) and (10,3) SWNTs, respectively. [11] We have also calculated the binding energies of those excitons. It should be noted that for E_{22} excitons, the MOD1-MOD2 oscillations in the binding energies are inverted, i.e., MOD2 tubes have larger binding energies than MOD1 tubes of similar diameter. In fact, in discrepancy with experiment, we find that (7,5) and (10,3) tubes should have E_{22} excitons with similar binding energies, even though the latter has a larger diameter. By using $\epsilon = 2.559$ we find the best possible "average" agreement with experiment: 0.54 eV for the (7,5) and 0.55 eV for the (10,3) nanotube.

In conclusion, we have determined the full diameter and chirality dependence of exciton binding energies, sizes, and splittings in semiconducting SWNTs. All these exciton properties have strong diameter and chirality dependences, with a distinct family behavior. Comparisons between theoretical and experimental binding energies should be exercised with care, by ackowledging environmental screening effects. Our results should provide an useful guide to the interpretation of recent and future experimental determinations of exciton binding energies and other properties.

---

[1] A. Jorio, R. Saito, J. H. Hafner, C. M. Lieber, M. Hunter, T. McClure, G. Dresselhaus, and M. S. Dresselhaus, Phys. Rev. Lett. **86**, 1118 (2001).

[2] S. M. Bachilo, M. S. Strano, C. Kittrell, R. H. Hauge, R. E. Smalley, and R. B. Weisman, Science **298**, 2361 (2002).

[3] C. D. Spataru, S. Ismail-Beigi, L. X. Benedict, and S. G. Louie, Phys. Rev. Lett. **92**, 077402 (2004).

[4] T. Ando, J. Phys. Soc. Jpn **66**, 1066 (1997).

[5] E. Chang, G. Bussi, A. Ruini, and E. Molinari, Phys. Rev. Lett. **92**, 196401 (2004).

[6] V. Perebeinos, J. Tersoff, and P. Avouris, Phys. Rev. Lett. **92**, 257402 (2004).

[7] H. Zhao and S. Mazumdar, Phys. Rev. Lett. **93**, 157402 (2004).

[8] F. Wang, G. Dukovic, L. E. Brus, and T. F. Heinz, Science **308**, 838 (2005).

[9] G. Dukovic, F. Wang, D. Song, M. Y. Sfeir, T. F. Heinz, and L. E. Brus, Nano Lett. **5**, 2314 (2005).

[10] J. Maultzsch, R. Pomraenke, S. Reich, E. Chang, D. Prezzi, A. Ruini, E. Molinari, M. S. Strano, C. Thomsen, and C. Lienau, Phys. Rev. B **72**, 241402(R) (2005).

[11] Z. Wang, H. Pedrosa, T. Krauss, and L. Rothberg, Phys. Rev. Lett. **96**, 047403 (2006).

[12] C. D. Spataru, S. Ismail-Beigi, R. B. Capaz, and S. G. Louie, Phys. Rev. Lett. **95**, 247402 (2004).

[13] V. Perebeinos, J. Tersoff, and P. Avouris, Nano Lett. **5**, 2495 (2005).

[14] E. Chang, D. Prezzi, A. Ruini, and E. Molinari, cond-mat/0603085 (2005).

[15] R. S. Knox, *Theory of Excitons*, vol. Suppl. 5 of *Solid State Physics* (Academic Press, New York, 1963).

[16] J. W. Brown and H. N. Spector, Phys. Rev. B **35**, 3009

(1987).

[17] T. Vuković, I. Milošević, and M. Damnjanović, Phys. Rev. B **65**, 045418 (2002).

[18] E. B. Barros and *et al.*, to be published (2006).

[19] R. Loudon, Am. J. Phys. **27**, 649 (1959).

[20] L. Bányai, I. Galbraith, C. Ell, and H. Haug, Phys. Rev. B **36**, 6099 (1987).

[21] K. Ohno, Theor. Chim. Acta **2**, 219 (1964).

[22] A. Jorio, C. Fantini, M. A. Pimenta, R. B. Capaz, G. G. Samsonidze, G. Dresselhaus, M. S. Dresselhaus, J. Jiang, N. Kobayashi, A. Grneis, et al., Phys. Rev. B **71**, 075401 (2005).

[23] R. B. Capaz, C. D. Spataru, P. Tangney, M. L. Cohen, and S. G. Louie, Phys. Rev. Lett. **94**, 036801 (2005).